Synthetic Clay Nanocomposite-Based Coatings Prepared by UV-Cure Photopolymerization

B. S. Shemper, J.-F. Morizur, M. Alirol, A. Domenech, V. Hulin, L. J. Mathias

School of Polymers and High Performance Materials, The University of Southern Mississippi, Hattiesburg, Mississippi 39406

Received 18 December 2003; accepted 24 February 2004
DOI 10.1002/app.20580
Published online in Wiley InterScience (www.interscience.wiley.com).

ABSTRACT: The effect of synthetic clay on the photopolymerization kinetics and coating properties of methyl α-hydroxymethylacrylate (MHMA) systems in the presence of novel hydroxylated dimethacrylate crosslinkers is reported. In the presence of clay earlier onset of autoacceleration was observed, high rates of polymerization were achieved, and high final overall conversions were reached. Higher rates and increase in conversions were also observed as the clay content increased in the medium. To increase compatibility between clay and polymer matrix the use of Jeffamines as polymer/clay compatibilizers, based on ion–dipole interactions between ethylene oxide units and clay ions, was also investigated. Nanocomposite-based films by photopolymerization of the mixtures coated on glass microscope slides were prepared and evaluated using X-ray and TEM. The absence of Bragg diffraction peaks in all nanocomposite films indicated loss of organization of the clay layers and formation of well-dispersed, exfoliated systems was confirmed by TEM. © 2004 Wiley Periodicals, Inc. J Appl Polym Sci 93: 1252–1263, 2004

Key words: photopolymerization; methyl α-hydroxymethyl acrylate (MHMA); crosslinking; laponite clay; coatings

INTRODUCTION

Polymer layered silicate nanocomposites have attracted great attention since Toyota and coworkers demonstrated a considerable enhancement of polymer properties by incorporating clays or layered aluminosilicate plateletlike structures into polymer matrices.[1–3] The dispersion of only a small amount of clay in the polymer, typically 3–5%,[4] confers dramatic improvements in polymer mechanical properties.[5,6] Improvements are observed in stiffness and strength, thermal stability, flame retardancy, solvent and UV resistance, and gas barrier properties.[7,8]

Several procedures have been used to produce polymer–silicate nanocomposites. These include melt compounding, solvent casting,[9] sol–gel methods, and *in situ* polymerization.[10] The morphologies of the systems obtained can usually be classified as either exfoliated or intercalated with some degree of aggregation.[11] Melt processing consists of blending a molten thermoplastic polymer with clay at high temperature and high shear, which can sometimes lead to thermodegradation during processing.[12] This may be overcome by using solution intercalation, which consists of swelling the clay in a solvent followed by addition of a solution of the polymer dissolved in the same solvent. Although removal of the solvent by evaporation leads to intercalated structures, large amounts of organic solvents are released during the process and excessive drying to remove trapped solvent is required.[12] Sol–gel processes have been recently used by Muh et al.[13] and by Moszner and coworkers[14] to prepare organic–inorganic hybrid materials through hydrolysis and condensation of organically modified silanes containing free-radically polymerizable methacrylate groups. These materials are particularly designed for dental applications, where properties such as flexural strength, modulus of elasticity, and volume shrinkage are important. When the *in situ* technique is used, the clay is swollen in the monomer and polymerization is carried out between and around the layers of clay. In some cases, however, cations present in the silicate, such as Na^+ or K^+, are exchanged for organic cations.[15] Alkylammonium ions are the most common compatibilizing agents used in the formation of polymer–clay nanocomposites. However, the reduction of organic modifiers in the synthesis of the nanocomposites has already been pointed out as a practical advantage.[16]

As an alternative to the procedures described above, the preparation of nanocomposites using UV-curing technology has only recently been reported.[12,17,18] Uhl et al.[17] demonstrated that the presence of clay reduced the cure time of urethane/acrylate-based films. More-

Correspondence to: L. Mathias (lon.mathias@usm.edu).
Contract grant sponsor: National Science Foundation; contract grant number: NSF-MRI Award 0079450.

over, Decker et al.[12] synthesized highly resistant nanocomposites based on polyurethane–acrylate systems using high solvent-free UV cure and pretreatment of the clay through surface alkylammonium cation exchange to render it more organophilic. Huimin and coworkers[19] also used photopolymerization to generate nanocomposites and found that noncrosslinked poly(methyl methacrylate) led to intercalated structures, whereas crosslinking during photopolymerization with *m*-cresol resin/*N,N*-hexa(methoxymethyl)-2,4,6-triamino-1,3,5-triazine (HMMM) system led to exfoliated structures. Advantages of using UV-curing to coat substrates include the low energy needed for the process, the high rates and highly efficient polymerization achieved, the ability to select the specific area to be cured, and the elimination of solvent reduced volatile organic pollution.[20]

Nanoscale particles typically used in the formation of nanocomposites are layered silicates such as natural montmorillonite or synthetic laponite.[21] Laponite® consists of particles of about 25 nm in diameter and 0.92 nm in thickness.[22] It has a layer structure composed of repeats of six octahedral magnesium ions sandwiched between two layers of four tetrahedral silicon atoms and an overall empirical formula $Na^{+}_{0.7}[(Si_8Mg_{5.5}Li_{0.3})O_{20}(OH)_4]^{-0.7}$.[23] Laponite has the advantages over natural clay of being chemically pure and free from crystalline silica impurities. It is also a very efficient rheology control agent for waterborne systems once it is rapidly dispersed, to give colorless, transparent, and highly thixotropic gels without the need for high shear mixing, elevated temperatures, or chemical dispersing agents.[24] Its small particle size and high transparency make it attractive for optical waveguide applications. Finally, laponite films can be used in the manufacture of electrically conductive, antistatic, and protective coatings at low cost.[25] Not surprisingly, several researchers have been studying the effect of laponite in nanocomposites. For instance, Inan and coworkers[26] recently investigated the effect of laponite in nylon-6 nanocomposites, focusing on the mechanism of char formation and flame-retardation behavior. Doeff et al.[27] recently reported that intercalation of poly(ethylene oxide) (PEO) into laponite, at a concentration of 0.7 g of polymer per g of Li–laponite, leads to an enhancement of the Li ion conductivity for applications such as rechargeable lithium batteries.

The behavior and morphology of systems containing PEO-based compounds as intercalating agents in nanocomposites have also been topics of recent investigation. Rheological studies of dispersions of laponite in water in the presence of relatively low molecular weight PEO (53,500 or 100,000 g/mol) have shown that the PEO polymers adsorb on single clay particles and do not bridge particles, thus decreasing the rate of gel formation of these systems.[28] Chaiko[29] recently attributed the adsorption of PEO polymers onto montmorillonite, saponite, and hectorite surfaces to entropic interactions resulting from partial replacement of hydration water associated with the exchangeable cations present in the clay galleries. The use of α,ω-diamine of poly(oxypropylene)-*b*-poly(oxyethylene)-*b*-poly(oxypropylene) (Jeffamines) as intercalating agents, resulting in an enlargement of the nanocomposite basal spacing by ion exchange of the quaternary ammonium end groups and sodium ions of montmorillonite clay, was also recently demonstrated.[30] The low percentage of ion exchange was attributed to a reduction of polymer mobility caused by the high affinity of the ethylene oxide units for the sodium ions on the clay surface.[30] The PEO chains tend to flatly "adsorb" on the clay surface because of its polar nature, whereas poly(propylene oxide)–diamines associate with the clay surfaces by tethered quaternary ammonium salts.[31]

In this work, we report results on the effect of clay on the photopolymerization kinetics and coating properties of methyl α-hydroxymethylacrylate (MHMA) systems. In addition, we explored the use of Jeffamines as polymer/clay compatibilizers by taking advantage of the ability of PEO to chelate adsorbed sodium ions on the clay surfaces. We also made use of the free amine groups by reacting them with acrylate functionalities of a crosslinker through Michael addition reactions.

EXPERIMENTAL

Materials

Laponite RD with a cation-exchange capacity (CEC; 55 mmol/100 g) was purchased from Southern Clay Products, Inc. (Gonzales, TX) and used as received. Ethanol (95%; AAPER Alcohol, Shelbyville, KY) and tetrahydrofuran (THF, HPLC grade; Fisher Scientific, Pittsburgh, PA) were also used as received. Methyl α-hydroxymethylacrylate was provided by Nippon Shokubai Co. (Tokyo, Japan), and used without further purification. 2,2-Dimethoxy-2-phenylacetophenone (Irgacure 651, Ciba Speciality Chemicals, Basel, Switzerland) was used as received. Tricaprylylmethylammonium chloride (Aliquat 336), 3-(acryloyloxy)-2-hydroxypropyl methacrylate (AHM), and 1,6-hexanediol diacrylate (HDDA) were purchased from Aldrich Chemical Co. (Milwaukee, WI) and used as received. A commercial polyether block copolymer of the type $H_2NCH(CH_3)CH_2[OCH(CH_3)CH_2]_y$-$[OCH_2CH_2]_x[OCH_2CH(CH_3)]_yNH_2$, with $x = 14$ and $y = 2$–3, was purchased from Huntsman Co. (Geismar, LA) under the trade name Jeffamine XTJ-501 and used without further purification. The hydroxylated dimethacrylate crosslinkers 3-(*N,N*-bis propionate diethylene glycol amino)-2-hydroxypropyl methacrylate

(B2), 3-(*N,N*-bis propionate triethylene glycol amino)-2-hydroxypropyl methacrylate (B3), and 3-(*N,N*-bis propionate adamantyl amino)-2-hydroxypropyl methacrylate (B4) were synthesized in our laboratory according to previously published procedures.[32]

Instrumentation

FTIR spectra were obtained using a Mattson 5000 spectrometer (Mattson Instruments, Madison, WI). Photopolymerizations were initiated with Irgacure 651 using a TA Instruments (Wilmington, DE) 930 differential photocalorimeter (DPC). Results of the DPC experiments were evaluated using Microcal Origin 4.1 and Microsoft Excel. Thermal analyses were performed on a TA Instruments (New Castle, DE) 2960 controlled by a Thermal Analyst 2100. Midangle X-ray diffraction (XRD) measurements were performed on a Siemens XPD-700P diffractometer (The University of Reading, Reading, UK) using Cu–K_α radiation in the 2θ range of 2–10°, at a sample detector distance of 30 cm. Specimens for transmission electron microscopy were prepared by cryosectioning the samples at an angle of 6° to the knife and at a speed of 1.5–3.5 mm/s on a Reichard-Jung Ultracut E microtome. The microtome chamber, glass knife, and samples were kept between 0 to −20°C. Ultrathin sections (~ 70 nm thick) were placed on copper TEM grids. The sections were viewed using a Zeiss EM 109-T electron microscope (Carl Zeiss, Jena, Germany) operating at 50 kV. Pencil hardness of coatings was performed according to ASTM test D3363-74 (pencil test).

Ion exchange

Organically modified laponite (OML) clay was obtained by ion exchange using laponite and tricaprylylmethylammonium chloride according to the procedure described below. Clay (1 wt %, 10 g), water (1 L), and 1.5 equivalents of surfactant (3.33 g) were stirred at 70°C overnight on a magnetic stir plate. The mixture was then hot-filtered using a Buchner filter with Whatman (Clifton, NJ) #2 filter paper; the slurry was then washed with 6 L of hot water (70°C) followed by drying under vacuum for 2 h. The dry clay was then ground into a powder using a mortar and pestle. The clay was next Soxhlet extracted with ethanol overnight under a nitrogen blanket; this extraction was repeated using tetrahydrofuran (THF). The final product (organically modified clay) was vacuum dried and ground using a mortar and pestle.

Preparation of coatings

Two methods of coating preparation were investigated. The first used organically treated clay (OML), whereas the second involved a compatibilizer and the untreated laponite clay. Coatings containing organophilic clay were synthesized by mixing the monomer MHMA (2.0 g), the crosslinker (AHM, HDDA, B2, B3, or B4) at a ratio of 10 wt % (0.2 g) relative to monomer, and the treated clay (0–10 wt %) overnight. The mixture obtained was stirred overnight, and 1 mol % (relative to total double bonds present) of the photoinitiator Irgacure 651 was added just before photopolymerizations.

In the second procedure, Jeffamine XTJ-501 containing approximately 14 PEO units was included in the coating mixture as a complexation agent with pristine laponite. The PPO-*b*-PEO-*b*-PPO diamine was initially mixed with excess crosslinker at a 1 : 2 wt % ratio and stirred overnight to ensure that all the amine groups of the Jeffamine reacted through Michael addition to the crosslinker before addition of the clay. In a typical procedure, Jeffamine (0.1 g, 0.11 mmol) and AHM (0.2 g, 0.93 mmol) were mixed overnight. MHMA (2.0 g, 17.24 mmol) and clay (0–0.2 g, 0–10 wt %) were then added and the system was once more mixed overnight, followed by the addition of 1 mol % of Irgacure 651 (0.0465 g) just before photopolymerization.

Photopolymerizations on glass

In a typical photopolymerization procedure, 1 mL of the coating mixture was placed on a glass microscope slide and spread with a small paintbrush to form a smooth film. The coated substrate was placed inside a polyethylene box containing inlet and outlet ports for nitrogen purge and a UV transparent lid. Nitrogen purge was maintained for 10 min before and throughout the photopolymerization, which was carried out for 90 min using a B 100-AP high intensity longwave UV lamp (UVP, Inc., Upland, CA) with radiation in the range of 315 to 400 nm (peaking at 365 nm) and light intensity of 8900 mW/cm^2 at 10 in. from the light.

Small-scale photopolymerization procedure (photo-DSC)

In a typical photo-DSC procedure, approximately 3.5 mg of the coating mixture was placed in a bottom-impressed and flattened aluminum DSC pan (~ 200 μm layer thickness). Heats of photoreactions were measured using a TA Instruments 930 Differential PhotoCalorimeter (DPC) equipped with a high-pressure mercury arc lamp. This unit emits radiation predominantly in the 220–400 nm range, and provides light intensity of 31 mW/cm^2 as measured by a UV radiometer capable of broad UV range coverage (UV Process Supply, Inc., Chicago, IL). The chamber of the DPC was purged with nitrogen for 10 min before irradiation and a nitrogen blanket was maintained throughout the reaction. Each set of experiments was

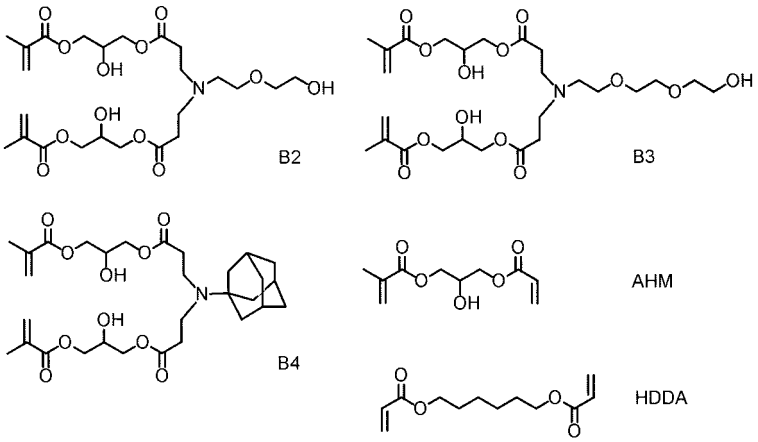

Figure 1 Structures of crosslinkers used in this work.

carried out sequentially so that light intensity during a given series of experiments would be relatively constant. Each sample was irradiated for 6 min at 30°C with the light shutter opening at 60 s after the beginning of data acquisition (i.e., onset of photocure occurred at 60 s). The enthalpy value, ΔH_{theor} = 13.1 kcal/mol, was used as the theoretical heat evolved for methacrylate double bonds, and for acrylate double bonds, the value of ΔH_{theor} = 20.6 kcal/mol was used.[33] The heat flux as a function of reaction time was monitored using DSC under isothermal conditions. Instantaneous rates of polymerization were calculated according to the following equation[34,35]:

$$\text{Rate} = \frac{(Q/s)M}{n(\Delta H_{pol}m)} \quad (1)$$

where Q/s is the heat flow/s, M is the molar mass of the monomer, n is the number of double bonds per monomer molecule, ΔH_{pol} is the heat released per mole of double bonds reacted, and m is the mass of monomer in the sample.

RESULTS AND DISCUSSION

We have recently been interested in both the synthesis and the photopolymerization behavior of novel monomers and crosslinkers prepared by Michael addition of amines to a commercial unsymmetrical difunctional compound containing one methacrylate and one acrylate group plus a pendant alcohol (AHM). Figure 1 shows the structures of AHM, hexanediol diacrylate, and some of the novel crosslinkers synthesized in our laboratories. The detailed procedure to make the hydroxylated dimethacrylate crosslinkers B2, B3, and B4 can be found elsewhere.[32]

One objective of this work was to investigate the effect of these novel crosslinkers compared to AHM (a mixed acrylate/methacrylate crosslinker) and hexanediol diacrylate (HDDA) at 10 wt % on the photopolymerization kinetics of methyl α-hydroxymethylacrylate (MHMA) systems. MHMA systems have been shown to possess very high polymerization rates both alone and in the presence of acrylate (HDDA) or methacrylate (HDDMA) crosslinkers. However, increasing the concentration of crosslinkers up to 2 mol % led to decreasing final conversions.[36] A second goal in this work was to incorporate synthetic clay in mixtures of MHMA and these crosslinkers to study its effect on the photopolymerization kinetics and conversions. A third goal was to prepare and evaluate nanocomposite-based films by photopolymerization of the mixtures coated on glass microscope slides. Two different methods were used to prepare the coating mixture, one involving ion exchange with a quaternary ammonium surfactant (Aliquat 336) and the second using pristine synthetic clay and a PEO-based diamine (Jeffamine XTJ-501) as a compatibilizer for the clay/polymer matrix.

To facilitate interpretation of the data we named the samples according to the procedure used for preparation of the coatings. OML samples were characterized by the presence of Aliquat-treated clay according to the first method of coatings preparation, whereas JC samples were prepared by the second method in which the Jeffamine was incorporated.

Effect of hydroxylated dimethacrylate crosslinkers on the photopolymerization of MHMA

Previous work in our group[32] showed that the photopolymerization of bulk hydroxylated dimethacrylate crosslinkers (B2, B3, and B4) gave very high reactions, with rates significantly higher than those of typical dimethacrylate monomers, such as HDDMA and approaching that of HDDA, while overall conversions reached 81% (±5).[32] Figure 2 shows the effect of the new crosslinkers, AHM, and HDDA on the poly-

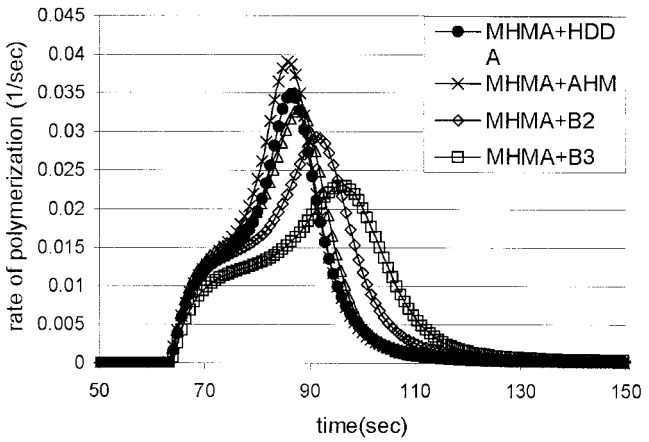

Figure 2 Polymerization rate versus time plots for MHMA at 30°C in the presence of 10 wt % of different crosslinkers; onset of photocure is at 60 s.

merization rate of MHMA at a crosslinker concentration of 10 wt %. The rates of MHMA polymerization in the presence of 10 wt % of the hydroxylated dimethacrylate crosslinkers (B2, B3, and B4) showed rates similar to those obtained with HDDA and AHM, with slightly slower onsets of autoacceleration. In addition, the final overall conversions achieved for the systems containing B2, B3, and B4 ranged from 72 to 75%, again similar to those for AHM and HDDA, as shown in Table I.

In agreement with previous results,[36] addition of a higher concentration of crosslinker (10 wt %) resulted in a decrease in final conversions compared to that of the neat MHMA system. This may be attributable to rapid microgelation, causing more monomer and pendant double bonds to be trapped in the network, making them less available for reaction and limiting conversion.

Effect of clay content on the photopolymerization kinetics of MHMA-based systems

Incorporation of high concentrations of layered silicates into a composite is difficult because of the large increase in viscosity of monomer–silicate mixtures at concentrations above 20 wt %. However, Zerda and coworkers[11] were able to incorporate large concentrations of organically modified layered silicates into poly(methyl methacrylate) (PMMA) through the use of supercritical CO_2 as a reaction medium. In this work, we were able to incorporate only 10 wt % of laponite into coating compositions while maintaining good dispersion and transparency. Two different methods were used to improve the compatibility with the polymer matrix. The first method used ion exchange of sodium cations on the surface of the clay sheets by the quaternary ammonium salt, tricaprylylmethylammonium chloride (Aliquat 336). Figure 3 shows the FTIR spectra of the pristine laponite, the surfactant alone, and the organically modified clay after exchange to 10 wt %. This amount of surfactant corresponds to 45% replacement of the CEC amount of cations present. An Si—O stretching band can be observed at 1047 cm^{-1} for the pristine clay [Fig. 3(a)] and is also observed in the OML [Fig. 3(c)]. Evidence of exchange with the surfactant can be clearly seen by the presence of CH_2 stretching peaks at 2933 and 2856 cm^{-1} in the FTIR spectrum of OML [Fig. 3(c)], by the band at 1465 cm^{-1} attributed to CH_2 bending, and also by the characteristic NH stretching as a broad band in the 3400 cm^{-1} region.

Ion exchange could also be quantified by thermogravimetric analysis (TGA). Figure 4 shows degradation curves of the clay before and after exchange with Aliquat. An estimated exchange of 10 wt % was calculated based on the difference between the residues at 600°C, indicating a CEC exchange efficiency of 45%.

The second modification method consisted of using a PEO-based diamine (Jeffamine XTJ-501) as a com-

TABLE I
Overall Conversions of MHMA with 10 wt % of Difunctional Crosslinkers

Crosslinker	Conversion (%)[a]
—	81 (2)[b]
AHM	73 (4)
HDDA	69 (7)
B2	75 (6)
B3	75 (4)
B4	72 (8)

[a] Values are the average of three trials with standard deviations given in parentheses.

[b] Value corresponds to overall conversion of neat MHMA in the absence of crosslinkers.

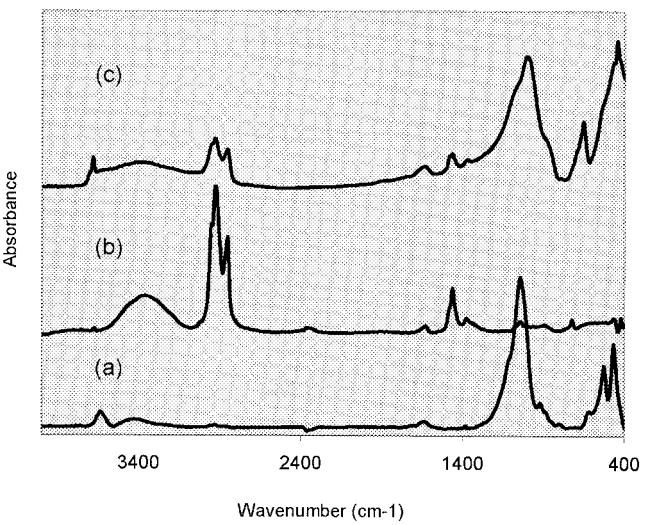

Figure 3 FTIR spectra of (a) pure laponite clay, (b) neat surfactant Aliquat 336, and (c) organically modified laponite (OML) clay.

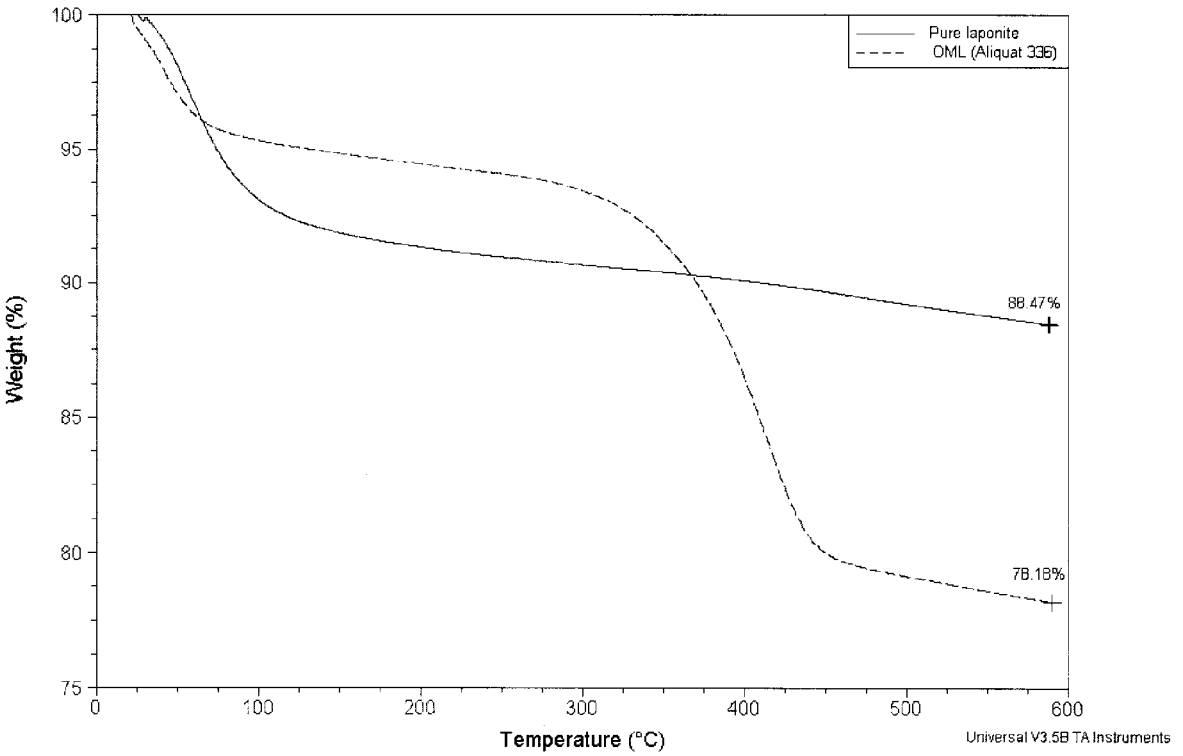

Figure 4 TGA curves of laponite clay before and after ion exchange with Aliquat 336 surfactant.

patibilizer for the pristine synthetic clay. The purpose of using an amino-terminal compatibilizer was twofold. First, we wanted to take advantage of the capability of the hydrophilic PEO chains to complex sodium ions on the clay surface. PEO has been shown to interact with the interlayer cations of clay in a manner similar to conventional PEO–salt complexes, which form "pseudo crown ether" type structures.[37] Aranda et al.[38] previously demonstrated that interactions between ethylene oxide units and interlayer cations of clay can be monitored by infrared spectroscopy, implying ion–dipole complexation. Figure 5 shows the FTIR spectra of pure laponite clay and a mixture of laponite with 50 wt % Jeffamine. In agreement with previous findings, split bands around 1347 and 1360 cm^{-1}, attributed to CH_2 stretching (indicated in the spectrum by the open arrow), were seen for the mixture of Jeffamine and clay and correspond to ion–dipole interactions between ethylene oxide units and clay ions.[38] Moreover, two bands near 950 and 860 cm^{-1}, attributed to rocking vibrations of methylene groups in the *gauche* conformation, also shown in Figure 5 by two arrows, can be related to those seen for PEO–salt complexes.[39] The absence of a peak near 1320 cm^{-1}, attributed to CH_2 stretching vibration of ethylene groups in the *trans* conformation, is further evidence of *gauche* conformations of the ethylene groups, and supports formation of a helical PEO conformation as required for cation complexation.[39]

Our second reason for using this Jeffamine is based on reaction of the terminal amines with the acrylate functionality of the crosslinker through a Michael addition. We recently reported efficient Michael addition of a variety of amines to the acrylate group of AHM and showed that this reaction can be monitored by ^{13}C-NMR spectroscopy.[32] By controlling the stoichiometry between the reactants, mono- or bisadducts may be prepared; use of this Jeffamine may allow

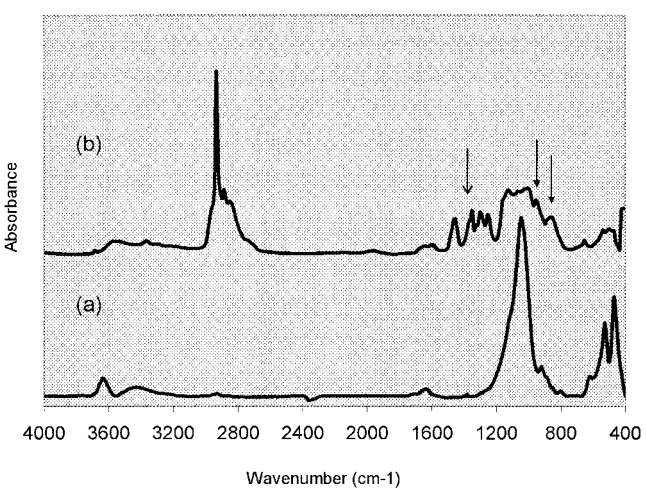

Figure 5 FTIR spectra of (a) pure laponite clay and (b) laponite clay with Jeffamine XTJ-501.

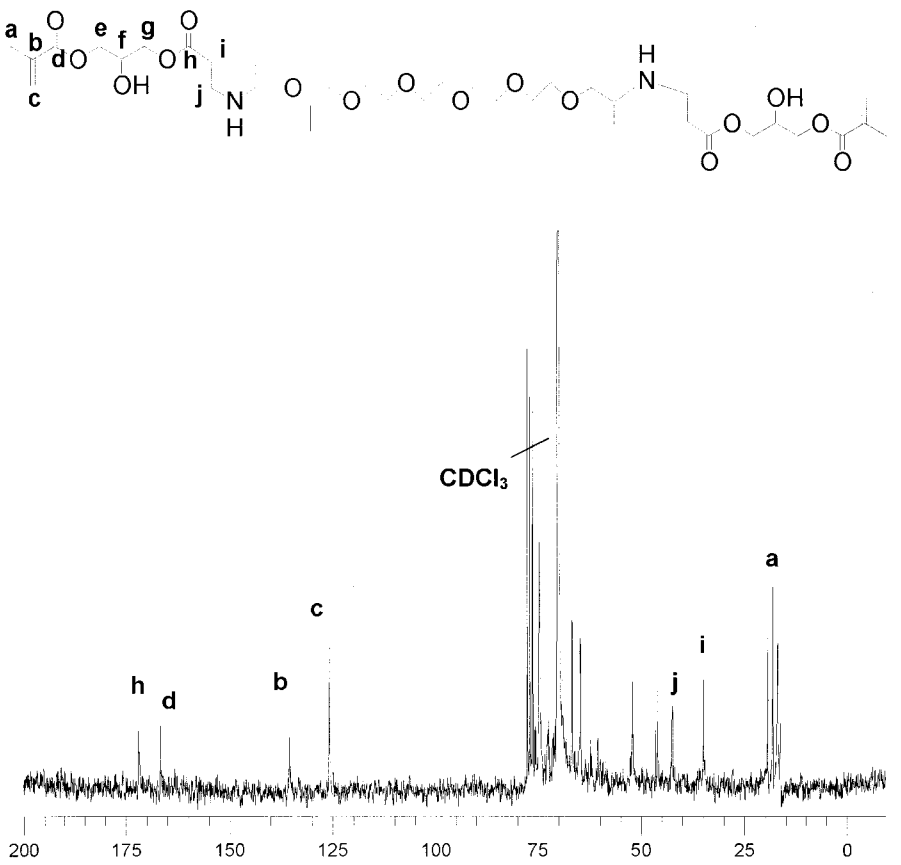

Figure 6 ^{13}C-NMR spectrum of the Michael adduct formed after addition of Jeffamine XTJ-501 to AHM at a 1 : molar ratio of reactants.

formation of a longer crosslinker (Fig. 6). Reaction between an equimolar ratio of Jeffamine and AHM should give the terminal dimethacrylate shown. Figure 6 also shows the ^{13}C-NMR spectrum of the crosslinker generated after overnight reaction of Jeffamine to AHM at a 1 : 1*M* ratio. The peaks observed, in comparison with those of mono- and bisadducts previously synthesized,[32] confirm that the major product is the mono adduct of each amine.

It should be noted that in the mixtures used for the photopolymerization studies, AHM or HDDA was present in excess (~ 8 : 1 mol ratio) compared to the Jeffamine. This ensured that all the amine functionality of the Jeffamine was reacted with the acrylate groups, yet free crosslinker still remained in the matrix to guarantee crosslinking throughout the sample. The two-step process involved initial formation of the Michael adducts, which were then mixed with monomer and pure clay to generate "pseudo crown ether" complexed sodium ions on the clay.

XRD spectroscopy was used to demonstrate successful organophilic treatment of the clay (Aliquat) and interaction between interlayer cations of the clay and the PEO units (of the Jeffamine). Expansion of the gallery dimensions of clay after exchange with the surfactant or incorporation of Jeffamine is confirmed by Figure 7, which gives the XRD patterns of pure clay, the OML, and the Jeffamine system.

The broad XRD peak observed for the pure laponite clay at a 2θ angle of 6.5° corresponds to an interlamellar spacing of 1.36 nm, as reported by others.[40] The difficulty in observing a sharp diffraction peak for the pure clay is attributed to the very small (20–30 nm) diameter of the clay platelets and to the poor long-range order caused by the aggregation of these platelets.[41] The diffraction peak shifted 2θ = 5.6° for the organically modified clay (OML) [Fig. 7(b)], signifying an increase of the interlayer distance of the clay sheets to 1.58 nm, whereas an increase to 2.14 nm was observed for the laponite plus Jeffamine [Fig. 7(c)]. The latter value is consistent with complexation between the cations of the clay and the PEO segments of the Jeffamine assuming a "pseudo crown ether" type of structure and leading to methacrylate termini oriented perpendicular to the clay surfaces, as schematized in Figure 8.

To investigate the effect of clay complexes on the polymerization rates and conversions of MHMA-based systems, photopolymerizations were carried out using various concentrations of clay (0, 1, 2, 3, 5, 7,

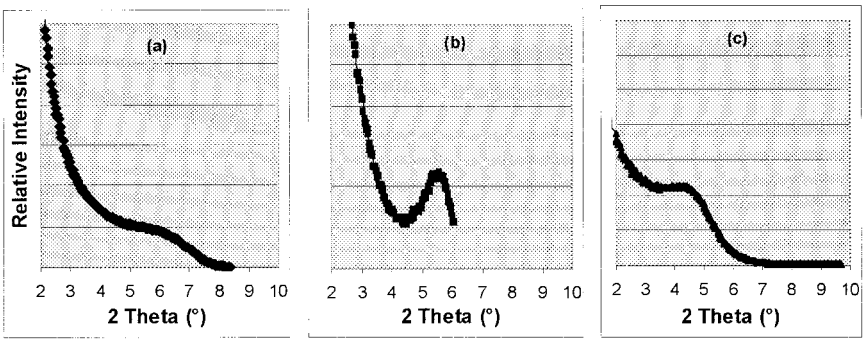

Figure 7 X-ray diffraction (XRD) patterns of (a) pristine laponite, (b) organically modified clay treated with Aliquat 336, and (c) laponite clay in the presence of Jeffamine XTJ-501.

and 10 wt %). Each mixture consisted of about 3 mg of methyl α-hydroxymethylacrylate (MHMA), 10 wt % of B2 or B3 used as crosslinkers, 1 mol % of Irgacure 651 used as photoinitiator, and different concentrations of treated clay. Both Aliquat exchanged clay (OML) and Jeffamine mixed with pure laponite were examined, with the Jeffamine added at 5 wt % relative to MHMA.

Figure 9 shows typical rates of polymerization for the systems containing MHMA, crosslinker B3, and different concentrations of OML. An earlier onset of autoacceleration in the presence of clay is clearly observed for all clay mixtures and rates were higher as the concentration of clay increased. Qualitative evaluation of tackiness of the coatings surfaces after predetermined time intervals indicated that "cure times" also decreased with increase in clay content, in agreement with the results of Uhl and coworkers.[17] One explanation for the higher rates of polymerization is the reduction of termination caused by the presence of high clay content in the reaction medium. This decrease in termination would increase radical concentrations and lead to earlier onsets of autoacceleration and higher rates of polymerization. That is, clay sheets could compartmentalize growing chains and increase overall viscosity of the reaction medium, both effects that would decrease termination events. Another explanation for the higher rates of polymerization at higher clay content is that monomolecular mode of chain termination between polymer chains and active spots on the surface of the clay will also be reduced at the initiator concentration used in these studies (0.09 mol/L), as suggested by Liu and coworkers.[42]

Final overall conversions of the polymerizations in the presence of clay were also higher, increasing significantly as the clay content increased in the medium (Table II). Increases in conversion could be attributable to lower termination rates, as was observed by Uhl et al.[17] for urethane/acrylate coatings containing different loadings of organically modified montmorillonite.

The rates of polymerization for systems containing MHMA, crosslinker B3, and different concentrations of pure laponite in the presence of Jeffamine are shown in Figure 10. Similar increases in polymerization rates as a function of higher clay content were seen, although onsets of autoacceleration were similar in all samples, as opposed to the system containing OML. This may be attributable to Jeffamine acting as a chain-transfer agent. Lower molecular weight polymer will thus be formed, delaying viscosity-induced

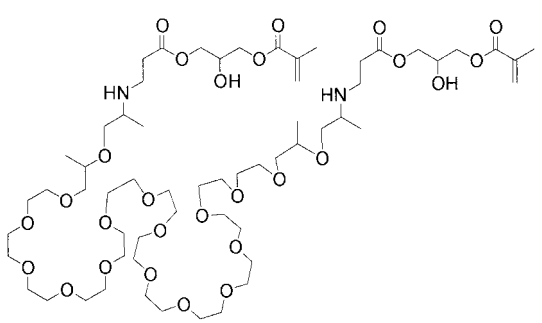

Figure 8 Schematic representation of the orientation of the proposed crown ether structure.

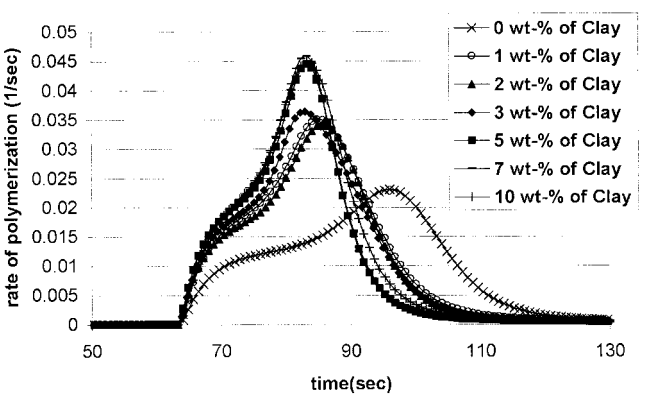

Figure 9 Rates of polymerization as a function of time for the MHMA-based system containing 10 wt % of B3 as a crosslinker and various concentrations of OML.

TABLE II
Final Overall Conversions for MHMA-Based Systems Photopolymerized in the Presence of Different Crosslinkers, and of Either Organically Modified Clay (OML) or Pure Laponite Combined with Jeffamine XTJ-501 as Compatibilizer (JC)

Clay concentration (wt %)	Overall conversion (%)[a]		
	MHMA/B3/OML	MHMA/B3/JC	MHMA/B2/JC
0	80 (4)	73 (2)	63 (4)
1	82 (1)	76 (2)	66 (3)
2	86 (3)	79 (2)	73 (4)
3	87 (4)	80 (3)	75 (4)
5	86 (4)	82 (4)	79 (2)
7	88 (4)	90 (3)	88 (4)
10	93 (3)	93 (4)	94 (4)

[a] Values are the average of three trials with standard deviations given in parentheses.

autoacceleration. This effect is better understood when both systems (OML and Jeffamine) are evaluated in the absence of clay, as seen by the curves in Figures 9 and 10 at 0 wt % clay. Both the rate of polymerization in the presence of Jeffamine and final conversion are reduced. Addition of clay leads to ether complexation with sodium cations, reducing the tendency for chain transfer alpha to the ether groups. This is especially evident at higher clay content (Table II), where most of the oligoethylene groups of the Jeffamine are complexed. This same behavior was observed for the MHMA-based system polymerized in the presence of Jeffamine and B2 as a crosslinker instead of B3 (Fig. 11). At higher clay content, chain transfer is not as important (fewer available hydrogens alpha to ethers) and the effect of clay in the systems prevails, increasing the polymerization rate and final overall conversions. In fact, calculation of the ratio of Na^+ to ether oxygens (based on CEC and Jeffamine structure and concentration) indicates that, for instance, at 10 wt % clay Jeffamine and sodium cations are present in equimolar amounts in the system, implying that most, if not all, of the sodium cations are complexed by oligoethylene groups; furthermore, these groups are not prone to chain transfer and a significant enhancement in polymerization conversion is achieved.

Nanocomposite films prepared by UV-cure polymerization

After the photopolymerization kinetics of the systems in the presence of clay were evaluated, nanocomposite coatings were prepared by UV photopolymerization on glass microscope slides to investigate the properties of the films formed. The coatings consisted of mixtures of MHMA; 10 wt % AHM, HDDA, B2, or B3 used as crosslinker; 1 mol % of Irgacure 651; and 10 wt % of either Aliquat-treated clay or pristine laponite clay, mixed with prereacted 5 wt % Jeffamine and crosslinker. The mixtures were coated on glass microscope slides and photopolymerizations carried out for 90 min under nitrogen flow, using a high-intensity UV lamp. The resulting films were qualitatively characterized for hardness and increases in the surface hardness were evident based on pencil hardness tests (Fig. 12). Repeatability was taken into account and each

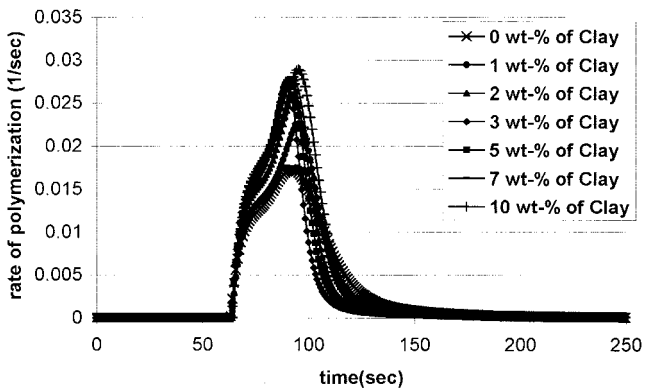

Figure 10 Rates of polymerization as a function of time for the MHMA-based system containing 10 wt % of B3 as a crosslinker, 5 wt % of Jeffamine XTJ-501, and various concentrations of pure laponite clay.

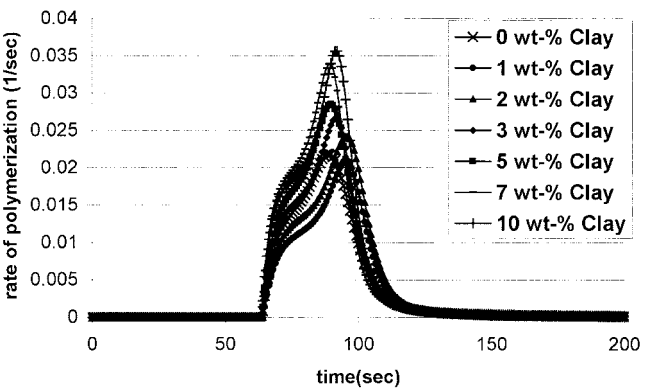

Figure 11 Rates of polymerization as a function of time for the MHMA-based system containing 10 wt % of B2 as a crosslinker, 5 wt % of Jeffamine XTJ-501, and various concentrations of pure laponite clay.

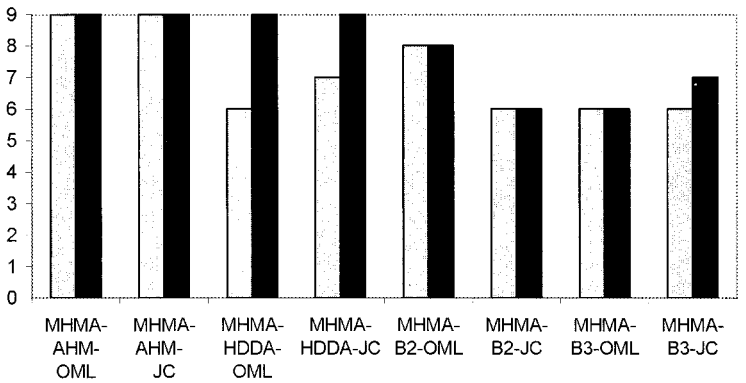

Figure 12 Pencil hardness results for MHMA coatings with 10 wt % of different crosslinkers in the absence of clay (dotted bars) and with 12 wt % of clay (dark bars). The type of clay treatment used (OML or JC) is indicated in the plot. Values in the *y*-axis are directly related to H levels of pencil hardness scale.

result of the pencil hardness tests given in Figure 12 corresponds to reproducible data collected for at least three separate coatings of the same composition.

The presence of AHM crosslinker in MHMA systems had a remarkable effect on the hardness of the coatings compared to other crosslinkers. All coatings prepared with AHM showed pencil hardness of 9H, significantly higher than that obtained for MHMA coatings formed in the absence of any crosslinker (6H). However, for films containing AHM the effect of clay on the scratch resistance could not be detected because of limitations of the pencil hardness test used. On the other hand, for systems containing typical crosslinkers used in the coatings industry, such as HDDA, a dramatic increase in scratch resistance was observed in the presence of clay. This is partially the result of good compatibility between clay particles and the polymer matrix, which results from interactions between clay sheets and the crosslinker HDDA either through covalent bonding (as for JC) or hydrophobic effects (as for OML). The type of crosslinker used in the coatings composition also had a pronounced effect on scratch resistance, as seen for results obtained for AHM-, B2-, and B3-containing systems. Scratch resistances of these coatings decreased in the order AHM > B2 > B3. The lower hardnesses obtained for coatings prepared with B3 or B2 are attributed to plasticization effects caused by higher flexibility of these crosslinkers compared to AHM. Moreover, the presence of clay did not have an effect on the scratch resistance of these coatings, likely because of the lack of interactions between the clay particles and these crosslinkers.

Removal of the films from the substrate, achieved by submerging the films in water, followed by peeling and air-drying, allowed structural characterization by X-ray spectroscopy as well as morphological evaluation by TEM. Figures 13 and 14 show the XRD patterns of nanocomposites films prepared by UV photopolymerization in the presence of OML and in the presence of Jeffamine-treated clay (JC), respectively. In Figure 13 a dashed line represents the peak position of the Aliquat-treated clay (OML), whereas in Figure 14 the diffraction peak corresponding to the mixture of Jeffamine and pure laponite was added to facilitate interpretation of the data. The absence of Bragg diffraction peaks in all nanocomposite films indicates loss of organization of the clay layers, which was confirmed by TEM. For example, the photomicrograph of the film of MHMA, 10 wt % HDDA, 5 wt % Jeffamine, and 10 wt % pure laponite is shown in Figure 15 and is representative of all the films evaluated. Overall, a well-dispersed and disordered morphology can be seen with only a few stacked silicate layers observed. This confirms that exfoliated systems were formed. An important factor contributing to exfoliated structures may be the size of the laponite clay particles used. It was previously shown that the layer stacking of clays with particularly small sizes, such as smectite (~ 50 nm), is more easily distorted mechanically, and gives broad diffraction peaks and small crystallite sizes in

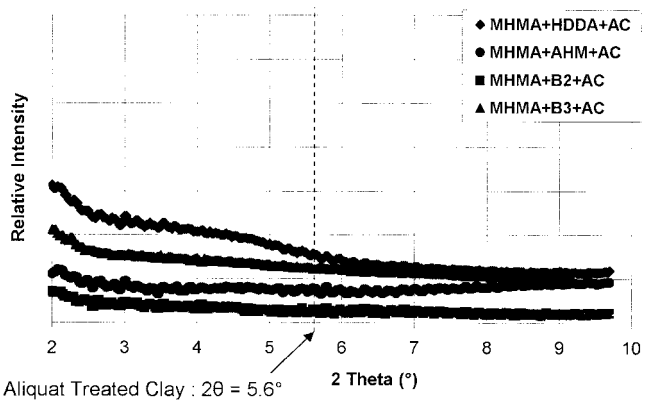

Figure 13 XRD patterns of the nanocomposite films prepared on glass microscope slides by UV photopolymerization of MHMA in the presence of 10 wt % of different crosslinkers and 10 wt % of OML (Aliquat-treated clay). The dashed line represents the peak position of the OML.

nanocomposites made from them.[43] This reduced order facilitates polymer penetration and nanocomposite formation. The smaller aspect ratio of the laponite clay used here may have contributed to formation of the well-dispersed, exfoliated systems obtained.

CONCLUSIONS

The effect of novel hydroxylated dimethacrylate crosslinkers (B2, B3, and B4) on the photopolymerization kinetics of methyl α-hydroxymethylacrylate (MHMA) systems was investigated and compared to those observed in the presence of AHM and HDDA. At 10 wt % rates of polymerization and final overall conversions achieved were similar in all systems. Synthetic clay was then incorporated at 10 wt % in mixtures of MHMA and these crosslinkers. In addition, two methods were used to increase compatibility between clay and polymer matrix and consisted of ion exchange by a quaternary ammonium salt and pseudo crown ether complexation of sodium ions by Jeffamines. Both methods were successful, as shown by the expansion of gallery dimensions of laponite detected by X-ray analysis. Jeffamines also provided terminal amine groups that reacted with acrylate functionalities of crosslinkers through Michael addition, as evidenced by ^{13}C-NMR spectroscopy. The effect of clay on the photopolymerization kinetics and conversions of MHMA-based systems containing the new crosslinkers was then investigated. In the presence of clay earlier onset of autoacceleration was observed, high rates of polymerization were achieved, and high final overall conversions were reached. Higher rates and increase in conversions were also observed as the clay content increased in the medium. One plausible explanation given for the higher rates and high conversions achieved was based on a combination of reduction of termination events and increase in viscosity caused by the presence of clay. The presence of Jeffamine in the systems led to some chain transfer alpha to the ether groups. However, in the presence of clay, rates of polymerization remained high and increased at higher clay contents. This was attributed to a competition between chain-transfer events and ether complexation, thus reducing the tendency for chain transfer.

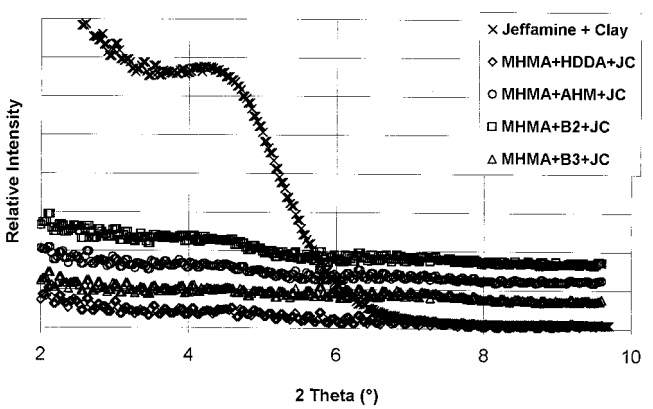

Figure 14 XRD patterns of the nanocomposite films prepared on glass microscope slides by UV photopolymerization of MHMA in the presence of 10 wt % of different crosslinkers, 5 wt % of Jeffamine XTJ-501, and 10 wt % pure laponite clay. The top left trace is for Jeffamine-treated clay.

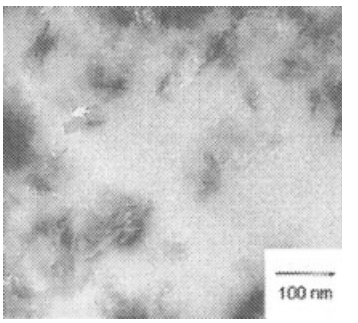

Figure 15 Transmission electron micrograph of the nanocomposite film prepared by UV photopolymerization of MHMA, with 10 wt % HDDA used as a crosslinker, 5 wt % Jeffamine, and 10 wt % laponite clay.

Nanocomposite-based films were prepared by photopolymerization of the clay-containing mixtures coated on glass microscope slides. Film properties were evaluated using X-ray and TEM. The absence of Bragg diffraction peaks in all nanocomposite films indicated the loss of organization of the clay layers and formation of well-dispersed, exfoliated systems was confirmed by TEM. The morphology obtained was likely caused by the small size of laponite clay particles used, which are usually characterized by disordered layer stacking and may have facilitated polymer penetration.

The authors thank Dr. Charles Hoyle for valuable discussions during interpretation of the photopolymerization data; the undergraduate students Jean-Francois Morizur, Matthiew Alirol, Angels Domenech, and Vincent Hulin for intensive collaboration; Maritza Abril, James Kopchick, and Dr. Kenneth Curry for assistance with TEM experiments; Dr. Demetrius McCormick, Camille Haynes, and Kirt Page for helping with the X-ray analyses; and Dr. Sonny Jonsson and Becker Acroma AB for collaboration.

Support by the NSF-MRI Award 0079450 NMR Grant is gratefully acknowledged.

References

1. Usuki, A.; Kawasumi, M.; Kojima, Y.; Okada, A.; Kurauchi, T.; Kamigaito, O. J Mater Res 1993, 8, 1174.
2. Usuki, A.; Kojima, Y.; Kawasumi, M.; Okada, A.; Fukushima, Y.; Kurauchi, T.; Kamigaito, O. J Mater Res 1993, 8, 1179.
3. Kojima, Y.; Usuki, A.; Kawasumi, M.; Okada, A.; Fukushima, Y.; Kurauchi, T.; Kamigaito, O. J Mater Res 1993, 8, 1185.

4. Zhu, J.; Wilkie, C. A. Polym Int 2000, 49, 1158.
5. Lan, T.; Pinnavaia, T. J. Chem Mater 1994, 6, 2216.
6. Wang, Z.; Pinnavaia, T. J. Chem Mater 1998, 10, 1820.
7. Bharadwaj, R. K.; Mehrabi, A. R.; Hamilton, C.; Trujillo, C.; Murga, M.; Fan, R.; Chavira, A.; Thompson, A. K. Polymer 2002, 43, 3699.
8. Tong, X.; Zhao, H.; Tang, T.; Feng, Z.; Huang, B. J Polym Sci Part A: Polym Chem 2002, 40, 1706.
9. Lim, S. K.; Kim, J. W.; Chin, I.; Kwon, Y. K.; Choi, H. J. Chem Mater 1989 2002, 14.
10. Jun, J.; Suh, K. J Appl Polym Sci 2003, 90, 458.
11. Zerda, A. S.; Caskey, T. C.; Lesser, A. J. Macromolecules 2003, 36, 1603.
12. Decker, C.; Zahouily, K.; Keller, L.; Benfarhi, S.; Bendaikha, T.; Baron, J. J Mater Sci 2002, 37, 4831.
13. Muh, E.; Marquardt, J.; Klee, J. E.; Frey, H.; Mulhaupt, R. Macromolecules 2001, 34, 5778.
14. Moszner, N.; Volkel, T.; von Clausbruch, S. C.; Geiter, E.; Batliner, N.; Rheinberger, V. Macromol Mater Eng 2002, 287, 339.
15. Argoti, S. D.; Reeder, S.; Zhao, H.; Shipp, D. A. Polym Prepr (Am Chem Soc Div Polym Chem) 2002, 43, 267.
16. Triantafillidis, C. S.; LeBaron, P. C.; Pinnavaia, T. J. Chem Mater 2002, 14, 4088.
17. Uhl, F. M.; Hinderliter, B. R.; Davuluri, P.; Croll, S. G.; Wong, S. C.; Webster, D. C. Polym Prepr (Am Chem Soc Div Polym Chem) 2003, 44, 247.
18. Xu, G. C.; Li, A. Y.; Zhang, L. D.; Wu, G. S.; Yuan, X. Y.; Xie, T. J Appl Polym Sci 2003, 90, 837.
19. Huimin, W.; Minghua, M.; Yongcai, J.; Qingshan, L.; Xiaohong, Z.; Shikang, W. Polym Int 2001, 51, 7.
20. Bongiovanni, R.; Montefusco, F.; Priola, A.; Macchioni, N.; Lazzeri, S.; Sozzi, L.; Ameduri, B. Prog Org Coat 2002, 45, 359.
21. Velde, B. Introduction to Clay Minerals: Chemistry, Origins, Uses, and Environmental Significance; Chapman & Hall: London, 1992.
22. Product information available at http://www.laponite.com/
23. Edwards, G.; Halley, P.; Martin, D.; Le, T. The Production of Novel Organo-Clay for Use in the Production of Nanocomposite Materials; The University of Queensland Chemical Engineering undergraduate thesis available online at http://www.cheque.uq.edu.au/ugrad/theses/2000/iitheses/G_Edwards.pdf (last updated on 09/09/2003).
24. Doyle, J.; Barlas, J. Polym Paint Colour J 1995, 185, 15.
25. Luyer, C. L.; Lou, L.; Bovier, C.; Plenet, J. C.; Dumas, J. G.; Mugnier, J. Opt Mater 2001, 18, 211.
26. Inan, G.; Patra, P. K.; Warner, S. B. Polym Mater Sci Eng 2003, 89, 725.
27. Doeff, M. M.; Reed, J. S. Solid State Ionics 1998, 113–115, 109.
28. Sardinha, H.; Bhatia, S. R. Polym Mater Sci Eng 2002, 87, 16.
29. Chaiko, D. J. Chem Mater 2003, 15, 1105.
30. Chou, C.; Shieu, F.; Lin, J. Macromolecules 2003, 36, 2187.
31. Lin, J.; Cheng, I.; Wang, R.; Lee, R. Macromolecules 2001, 34, 8832.
32. Mathias, L. J.; Shemper, B. S.; Alirol, M.; Morizur, J. Macromolecules, in press.
33. Anseth, K. S.; Wang, C. M.; Bowman, C. N. Macromolecules 1994, 27, 650.
34. Horie, K.; Otagawa, A.; Muraoka, M.; Mita, I. J Polym Sci Part A: Polym Chem 1975, 13, 445.
35. Miyazaki, K.; Horibe, T. J Biomed Mater Res 1988, 22, 1011.
36. Smith, T.; Shemper, B. S.; Nobles, J. S.; Casanova, A. M.; Ott, C.; Mathias, L. J. Polymer 2003, 44, 6211.
37. Shen, Z.; Simon, G. P.; Cheng, Y. Polymer 2002, 43, 4251.
38. Aranda, P.; Ruiz-Hitzky, E. Acta Polym 1994, 45, 59.
39. Papke, B. L.; Ratner, M. A.; Shriver, D. F. J Phys Chem Solids 1981, 42, 493.
40. Kubies, D.; Jerome, R.; Grandjean, J. Langmuir 2002, 18, 6159.
41. Zhu, H. Y.; Lu, G. Q. Langmuir 2001, 17, 588.
42. Liu, G.; Zhang, L.; Qu, X.; Wang, B.; Zhang, Y. J Appl Polym Sci 2003, 90, 3690.
43. Maiti, P.; Yamada, K.; Okamoto, M.; Ueda, K.; Okamoto, K. Chem Mater 2002, 14, 4654.